Exposure of the Human Body to Professional and Domestic Induction Cooktops Compared to the Basic Restrictions

Andreas Christ,[1]* René Guldimann,[2] Barbara Bühlmann,[1] Marcel Zefferer,[1] Jurriaan F. Bakker,[3] Gerard C. van Rhoon,[3] and Niels Kuster[1,4]

[1]*Foundation for Research on Information Technologies in Society (IT'IS), Zurich, Switzerland*
[2]*State Secretariat for Economic Affairs (SECO), Zurich, Switzerland*
[3]*Erasmus MC-Daniel den Hoed Cancer Center, Department of Radiation Oncology, Rotterdam, The Netherlands*
[4]*Swiss Federal Institute of Technology (ETHZ), Zurich, Switzerland*

We investigated whether domestic and professional induction cooktops comply with the basic restrictions defined by the International Commission on Non-Ionizing Radiation Protection (ICNIRP). Based on magnetic field measurements, a generic numerical model of an induction cooktop was derived in order to model user exposure. The current density induced in the user was simulated for various models and distances. We also determined the exposure of the fetus and of young children. While most measured cooktops comply with the public exposure limits at the distance specified by the International Electrotechnical Commission (standard IEC 62233), the majority exceeds them at closer distances, some of them even the occupational limits. The maximum current density in the tissue of the user significantly exceeds the basic restrictions for the general public, reaching the occupational level. The exposure of the brains of young children reaches the order of magnitude of the limits for the general public. For a generic worst-case cooktop compliant with the measurement standards, the current density exceeds the 1998 ICNIRP basic restrictions by up to 24 dB or a factor of 16. The brain tissue of young children can be overexposed by 6 dB or a factor of 2. The exposure of the tissue of the central nervous system of the fetus can exceed the limits for the general public if the mother is exposed at occupational levels. This demonstrates that the methodology for testing induction cooktops according to IEC 62233 contradicts the basic restrictions. This evaluation will be extended considering the redefined basic restrictions proposed by the ICNIRP in 2010. Bioelectromagnetics 33:695–705, 2012. © 2012 Wiley Periodicals, Inc.

Key words: induction cooking; ELF magnetic field exposure; compliance testing; exposure of the fetus; exposure of adults and children

INTRODUCTION

Induction cooktops have been replacing traditional gas stoves, particularly in professional kitchens. In comparison to traditional electric stoves, induction cooktops yield better energy efficiency and offer more flexible heating control, while avoiding the open flame and leakage risks from gas stoves. Initial studies on the exposure of the human body in the close environment of induction cooktops were not conclusive [Yamazaki et al., 2004]. However, a detailed experimental evaluation by Viellard et al. [2006] demonstrated that the incident B-field exposure can exceed the reference levels posed by the International Commission on Non-Ionizing Radiation Protection (ICNIRP) [ICNIRP, 1998a] by more than a factor of 30 at close distances by devices shown to

be compliant at the measurement distance of 300 mm defined by the International Electrotechnical Commission (IEC) [IEC, 2005]. A recent publication by Kos et al. [2011] quantifies the user exposure to a specific induction cooktop. While the authors do not observe violations of the exposure limits for the evaluated cooktop, they mention that the induced current density of the ICNIRP 1998 guidelines "could exceed the basic restrictions for induction cooktops in compliance with the IEC 62233 standard."

Many countries have adopted the safety guidelines issued by the ICNIRP in 1998, as well the 2005 IEC measurement standard (IEC 62233). Besides the derived reference levels, the ICNIRP guidelines also define basic restrictions for the actual exposure of the human body. In the ICNIRP 1998 guidelines, the latter were introduced in terms of the induced current density for the head and the trunk in order to protect against peripheral nerve stimulation. A clarification of the guidelines issued shortly after their original publication, however, reduces the applicability of these restrictions to tissues of the central nervous system (CNS), that is, the brain and spinal cord [ICNIRP, 1998b]. No limits are provided for other body tissues. Due to this uncertainty, some regulators, for example, Switzerland, require that the basic restrictions on the current density be met in all tissues of the trunk and head as originally stated. In the recently published guidelines on low frequency exposure, the ICNIRP abandons the assessment of the averaged current density in favor of restrictions on the electric field in the body averaged over a cubical volume of 2 mm × 2 mm × 2 mm [ICNIRP, 2010]. Separate limits are defined for the CNS tissues of the head and for all other tissues of the body for frequencies up to 1 kHz. Above 1 kHz, the basic restrictions are identical. Since these limits have not yet been adopted by regulators, they are not investigated within this article but will be the subject of a follow-up study.

Although a detailed exposure analysis was not carried out by Viellard et al. [2006], a simple analytical approximation showed that violations of the basic restrictions on the induced current density in the body of a person in the immediate environment of the stove are likely. This study aims to close the gaps regarding compliance with the basic restrictions that are currently imposed in many countries. This will be done by assessing the current density in the human body using a set of anatomical high-resolution models of adults of different heights and body mass indices. In addition, models of a pregnant woman in different gestational phases and young children whose heads are at the same height as the cooking

zones will be evaluated. The incident fields are modeled using the results of an experimental evaluation of professional cooktops in different gastronomic kitchens and of the two domestic cooktops and the portable cooktop evaluated by Viellard et al. [2006].

In detail, the objectives of this study are to complement the analysis of the three domestic devices used in Viellard et al. [2006] by the experimental evaluation of the B-fields of 13 different professional cooktops at different installation sites; numerically assess the induced current density in users and bystanders using different anatomical models of adults, children and pregnant women in typical and worst-case situations and postures; and discuss the exposure from the specific devices and the consistency of the product standard IEC 62233 with the ICNIRP 1998 basic restrictions.

METHODS

Experimental Methods

The spatial distribution and the frequency spectra of the B-fields of 13 professional induction cooktops were measured using a low frequency E- and H-field probe (EHP-200, Narda Safety Test Solutions, Hauppauge, NY) within a frequency range from 9 to 400 kHz. The spatial distribution was sampled in steps of 90 mm × 90 mm over a surface ranging from 625 to 1795 mm above the floor (z-axis) and −450 to 360 mm from the left to right (y-axis) with zero as the center of the cooktop. These measurements were taken at distances of 0 and 300 mm from the front edge of the cabinet that houses the cooktops. The first distance can be regarded as the closest a user can stand without bending over the device, whereas the latter can be regarded as a distance typical of passers-by while the cooktop is operational. Additional measurements at distances of 50, 100, 150, 200, and 250 mm were taken at the location of the field maximum observed when measuring the spatial distribution at 0 mm. Figure 1 shows an overview of the references of the measurement distances used in this study. For the evaluation of compliance of the B-fields with safety limits, IEC 62233 defines a position 300 mm from the edge of the cooktop [IEC, 2005]. This position depends on the dimensions of the cabinet and the mounting position of the cooktop and is therefore different for all evaluated devices. Supplementary Table I shows an overview of these distances. The B-fields at the distance of 300 mm are evaluated by interpolating the fields at the measured distances listed above using a curve fit.
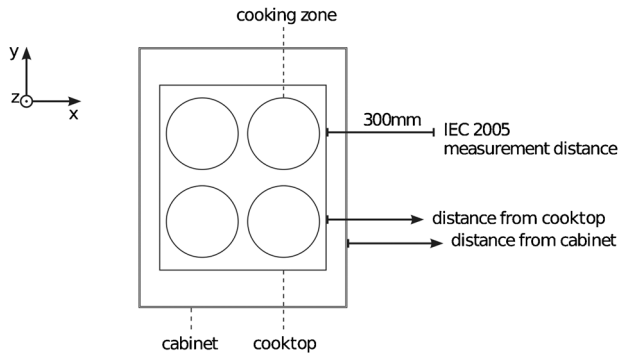
Fig. 1. Sketch of an induction cooktop with four integrated circular cooking zones built into a cabinet. The measurement distances are 0 and 300 mm from the edge of the cabinet.

For the accurate positioning of the probe, a foam plastic wall with mounting holes was used (Fig. 1 in the Online Supplementary Material). The mechanical stability of the wall was considered when determining the number and the spatial density of the holes. The orthogonal current loops of the EHP-200 probe, which pick up the vector components of the B-field, are not concentric. They have a diameter of approximately 31 mm. The center of the loop of the z-component of the B-field, which is the dominant component for all the cases investigated here, has an offset of approximately 42 mm from the frontal surface of the probe case. This offset was considered when normalizing the field distribution of the numerical model to the measured cases.

Only fields in the front of the cooktops were evaluated. During the measurements, the active cooking zones were loaded with a reference vessel (270 mm diameter, 145 mm height) that was filled with 3 L of water. The water that evaporated during the measurements was refilled. The cooking zones were operated at maximum power. Only the maximum values of the power control cycles of the cooking zones were considered. The decay of the B-fields with distance was assessed at the location of the maximum of each device. Additional measurements were carried out with different vessels and off-center positions on the cooking zone. The impact of the loading on the B-field strength used for the dosimetric evaluations was added as an offset in the dosimetric evaluation. Eleven of the 13 cooktops (#1–#11) were fixed installations. Cooktop #12 was a portable device with a single cooking zone, and Cooktop #13 was a wok installed in a fixed housing.

In addition to the professional cooktops, the three domestic devices referred to as cooktops #14–#16, originally evaluated in Viellard et al. [2006], were also used for the dosimetric assessment of the

current density induced in the user. These devices were measured with an ELT-400 probe (Narda Safety Test Solutions) positioned using a DASY 4 Dosimetric Assessment System (Schmid & Partner Engineering, Zürich, Switzerland).

Numerical Exposure Modeling

In the low frequency range, where the relevant dimensions of the computational domain are significantly smaller than the free space wavelength, the magnetic vector potential **A** can be assumed to be decoupled from the electric field **E**. As a consequence, **A** can be calculated using Biot–Savart's law, and since the divergence of the current density vanishes and conduction currents are dominant in the human body for the application in this article, **E** can be calculated from the scalar potential Φ, which is given by: $-\nabla \cdot \sigma \nabla \Phi = j\omega \nabla \cdot (\sigma A)$ with σ as the tissue conductivity and ω as the angular frequency of the fields of the induction cooktop. **A** is calculated using a Biot–Savart solver, and the finite element method is used to solve for Φ. The Biot–Savart solver and the finite element algorithm are implemented in SEMCAD $\times$ 14.2 (Schmid & Partner Engineering). Unlike typical finite element methods, the implementation used here operates on rectilinear meshes like the finite-difference time-domain method [Taflove and Hagness, 2000]. In this way, complex anatomical models can easily be rendered by adapting the mesh resolution. A description of the low frequency solver and its validation can be found in Capstick et al. [2008].

Alternative methods for the calculation of the exposure of the human body were proposed in the past, which evaluated the scalar potential Φ using finite-difference approximations [Dawson et al., 1997; Liu et al., 2003], frequency-scaling [Gandhi and Chen, 1992], or modeling the human body as an impedance network [Orcutt and Gandhi, 1988]. The recent study by Kos et al. [2011] applies the finite element method used here.

The dosimetric results were assessed in terms of the current density maximum (peak current density) in different body tissues. The ICNIRP 1998 guidelines define the basic restrictions for the current density as the average over a cross section of 1 cm^2. The orientation of the cross section is perpendicular to the currents flowing through it. An algorithm to calculate this average current density was implemented for the post-processing of the simulation results. The algorithm determines the direction of the current density vector on each grid node. The current density is then integrated on a circular surface that is perpendicular to this vector and has the required

dimensions of 1 cm^2. The maximum of the values of all grid nodes is reported as the peak average current density. The numerical uncertainty with respect to grid resolution and size of the averaging surface is shown in Tables V and VI of the Online Supplementary Material.

The evaluation of the average current density can be restricted to particular body tissues. This is used to quantify the exposure of the brain and spinal cord, for example. In the following sections of this article, the brain and the spinal cord will be referred to as the CNS. In a recent publication by Dimbylow [2008], problems were reported for the evaluation of the average current density in the spinal cord because the cross sectional area of the spinal cord can be less than 1 cm^2 for significant parts along its length. If the evaluation of the current density is restricted to particular tissues (e.g., the CNS) such that the required cross section cannot be reached, only the contributions of current densities from those tissues are considered for the averaging.

EXPERIMENTAL RESULTS

The spatial distribution of the B-field at the cabinet edge of one of the measured cooktops is shown in Figure 2 as an example, together with its spectral content. For all measured cooktops the dominant spectral component lies at approximately 20 kHz. Most cooktops show even and odd harmonics throughout the entire measurement range (up to 400 kHz). Their amplitudes are always a factor of 10 or more below the amplitude of the fundamental frequency. Therefore, the higher harmonics are not

considered for the numerical assessment of the induced current density. Only a harmonic signal of 20 kHz is used.

As the probe reference point has an offset with respect to the center of the loop for the z-component, the correction for the offset and its uncertainty have been determined as follows. The B-field of a generic cooking zone model was integrated over the loop diameter and compared to the B-field at the probe reference point as a function of the distance to the cooking zone. The ratio of the integrated B-field and the B-field at the reference point changes as a function of the field gradient and therefore depends on the distance to the cooking zone. The mean value for the offset correction is 1.1 (averaging over all measured positions along the z-axis). The maximum deviation from this average is 1.1 and is considered in the uncertainty evaluation (Supplementary Table IV) as a rectangular distribution.

Figure 3 shows the maximum B-field amplitudes of the 13 professional induction cooktops evaluated directly at the cabinet edge and at a distance of 300 mm from the cooktop edge at their operational frequency of 20 kHz. The positions ($y - z$ coordinates as specified in Figs. 1 and 2) of the maxima in the plane at the cabinet edge and in the plane at a distance of 300 mm coincide within the spacing of the probe mounting positions in the measurement wall (Fig. 1 in the Online Supplementary Material).

At 300 mm, most devices were found to be compliant with the ICNIRP 1998 reference level of 6.25 μT for the general public, although their field strengths vary by more than a factor of 30. Immediately in front of the cabinet (0 mm), all but two
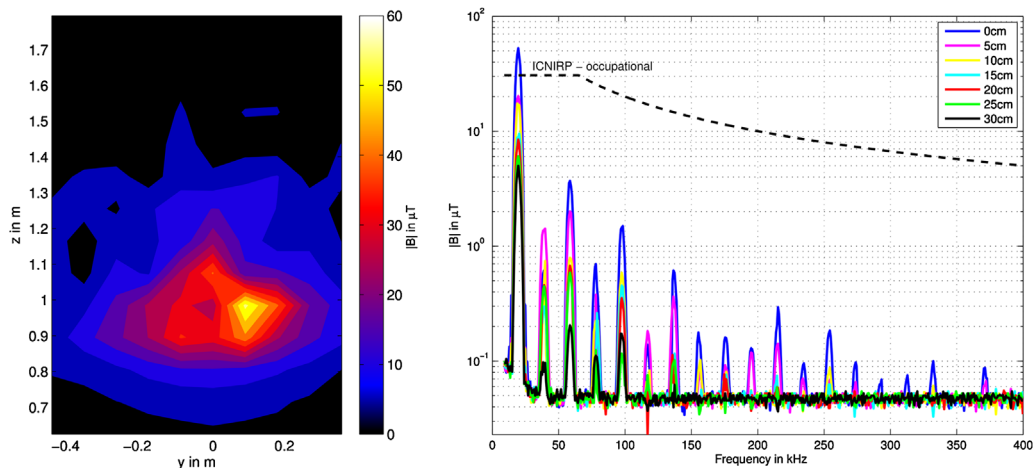

Fig. 2. Measured B-field of one of the cooktops normalized to the occupational ICNIRP limit (30.7 μT). Left: frontal plane at the cabinet edge; right: spectrum of the signal at different distances.
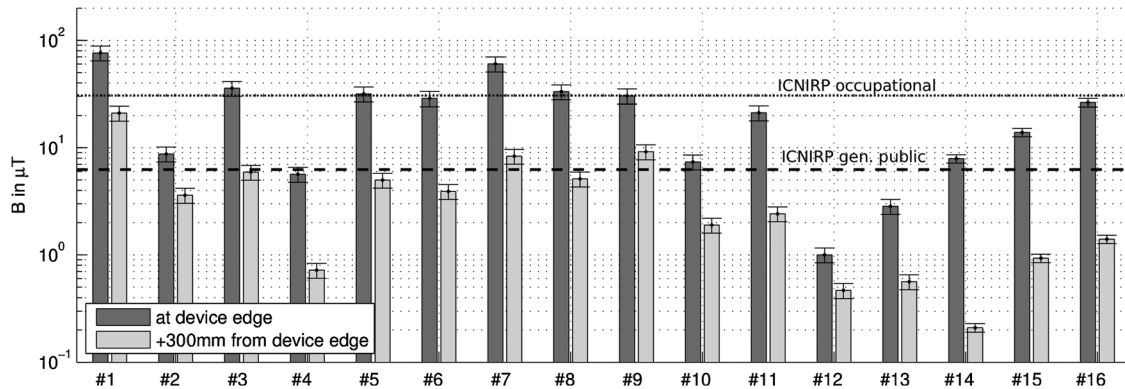
Fig. 3. Measured maxima of the B-field of 16 induction cooktops (professional and domestic) at the cabinet edge and 300 mm from the edge of the cooktop at their operational frequency of 20 kHz (not considering harmonics). Error bars indicate the measurement uncertainty ($k = 1$) of 16% (1.3 dB, devices $\#1$–$\#13$) and 9% (0.8 dB, devices $\#14$–$\#16$) as given in Supplementary Table IV, excluding the contribution of the numerical representation of the measured devices.

devices are within the more relaxed occupational limits of 30.7 µT; significant differences between the professional (#1–#13) and domestic devices (#14–#16) could not be observed. Also, the maximum B-field amplitudes could not be correlated with the nominal power of the different devices. The power consumption was not monitored during the measurements because the primary source of exposure is the magnetic field. The magnetic field amplitude does not only depend on the power but also on the complex impedance of the loaded coil.

In addition, the impact on the B-field was evaluated for loading conditions with different vessels, which were also positioned off the center of the cooking zone. Vessels that are not particularly specified for use with induction cooktops were included as well. For almost all devices, increased field strengths could be observed with respect to the standard configuration specified in IEC 62233. Supplementary Table II summarizes the results. In the worst case, an increase of more than a factor of 4.5 was found (#14).

NUMERICAL EXPOSURE EVALUATION

Exposure Configurations

For the assessment of the current density induced in the body, six non-pregnant and three pregnant anatomical whole-body models were selected for the dosimetric analysis by considering the body mass range of people working in professional kitchens. Models of young children were also included. All models are based on the computer-aided design representation of the organ surfaces and up to 80 different tissue types are represented (up to 17 in

the fetus models[1]). The non-pregnant models were developed from magnetic resonance (MR) images of volunteers [Christ et al., 2009, 2010]. Their details are: "Fats": male, 37 years, 1.78 m, 120 kg; "Duke": male, 34 years, 1.74 m, 70 kg; "Ella": female, 26 years, 1.60 m, 58 kg; "Louis": male, 14 years, 1.65 m, 50 kg; "Thelonious": male, 6 years, 1.17 m, 20 kg; "Roberta": female, 5 years, 1.08 m, 18 kg.

The models of the pregnant woman are based on the model "Ella." For the development of the fetus and womb during the different gestational phases, images from various sources were used. The fetus models represent the 3rd, 7th, and 9th gestational month. Their masses are 15, 1700, and 2700 g, respectively. For the model in the 3rd month, a generic model based on images in the available scientific literature, for example, Levine [2005], was integrated into the womb of the model "Ella," which was scaled in order to accommodate the fetus. The outer shape of the model was not changed. For the development of the model in the 7th month, MR images of the torso of a pregnant woman were segmented and integrated into the model. The model of the 9th month is based on that of the 7th month, but the fetus model was replaced by a model of a scaled newborn [Petoussi-Henss et al., 2002]. The dimensions of the abdominal region of the mother model were increased in order to accommodate the larger

---

[1]The fetal tissues include bladder, bone, brain, eyes, fat, gall bladder, heart, intestines, kidney, liver, lung, muscle, subcutaneous adipose tissue, skin, spinal cord, spleen, and stomach. It should be noted that not all three fetus models distinguish all tissues.

fetus. Figure 2 of the Online Supplementary Material shows an overview of all anatomical models used in this study. The tissue conductivities for the simulations at 20 kHz are based on Gabriel et al. [1996].

The current densities in the bodies of the anatomical models were simulated using a generic cooking zone model that could be adapted to the incident fields of the measured devices. For the four non-pregnant models, the cooking zone was placed at distances of 10–310 mm from the body in steps of 100 mm (measured horizontally from the rim of the cooking zone to the closest point of the skin). It was placed both in front of and behind the models. The default height of the cooking zone model was 850 mm above ground. For the assessment of the uncertainty of the results with respect to the body height and position of the user, the height of the cooking zone was also varied in steps of ±100 mm and moved to the left in steps of 100 mm. The results of these evaluations are considered only in the uncertainty budget (Tables IV–VI in the Online Supplementary Material) and not reported individually. For the evaluation of the exposure of the two models of young children, the same configurations as for the adults were used but the height of the coils was adjusted to their foreheads. This corresponds to body heights of approximately 1.0 m and to an age range of 3–4.5 years for boys and girls [Kromeyer-Hauschild et al., 2001]. Figure 3 in the Online Supplementary Material shows the different configurations. They were used for the evaluation of the uncertainty and variability of the exposure (Tables IV–VI in the Online Supplementary Material).

Additional scenarios were analyzed in order to assess the effect of the posture of the body when operating the induction cooktop. The models "Duke" and "Ella" were bent over the hob at angles of 22.5° and 45°. For these configurations, the closest distance from the rim of the cooking zone to the skin of the model was also 10 mm. Again, these evaluations were considered only in the uncertainty budget. For the assessment of the current density induced in the fetus and in the womb of the pregnant women models, the cooking zone was placed at three different heights in the center of the abdomen. Again, the minimum distance to the skin was 10 mm. The distance increased in steps of 100 mm, and the height changed by ±100 mm. The changes in exposure for these positions were considered in the evaluation of the uncertainty and variability (Tables IV–VI in the Online Supplementary Material). In addition, the hands of the model "Duke" were positioned above the center and above the rim of the cooking zone. The vertical distances of the hand to the cooking

zone were 50, 100, and 150 mm. Two horizontal positions were analyzed (above the center and above the rim). The results of the evaluation of the exposure of the hands are discussed below.

Modeling of the Incident B-Fields

In the experimental evaluation of the B-fields, a number of cooktops were evaluated both under the loading conditions defined by IEC 62233 [IEC, 2005] and with a large series of different vessels replicating several realistic exposure scenarios. Differences in the field distribution in the measurement planes were observed due to different cooking zone configurations or loading with different vessels, for example (Supplementary Table II). These differences would not permit the accurate evaluation of a particular cooktop without significant modeling and validation efforts under a number of representative loading configurations. Because it is not the objective of this article to evaluate the compliance of particular induction cooktops, the most generic approach has been chosen to model the spatial characteristics of the magnetic field distribution. Thus, the amplitude range of the induced current density can be quantified for realistic exposure scenarios. The applied cooking zone model consists of ten concentric loops with a constant current. The distance between the loops is 10 mm. In the radial direction (r), the B-field amplitude decays approximately with $1/r^3$ [Yamazaki et al., 2004].

In order to assess the exposure of the anatomical models for the B-field amplitudes of the different measured devices (Fig. 3), the current density, which was evaluated using the generic cooking zone at distances from 10 to 310 mm in the x-direction from the coil (Fig. 1), was scaled to match the B-field amplitudes of the measured devices at different measurement distances and the actual distance between the coil of the cooking zone and the measurement location. For each measured device, a scale factor was derived. Figure 4 shows the B-fields for each of the devices fitted to the B-field of the generic cooking zone at the different locations of the measurements.[2] Considering the distances to the rim of the cooking zone, the agreement of the measured values at all evaluated distances in the x-direction is generally satisfactory using a single scale factor for each device. The uncertainty of the representation of the amplitudes and field decay of the measured cooktops

---

[2]Between two and eight points in the x-direction were evaluated depending on the different devices. Up to four measurement points per device are shown in Figure 4.
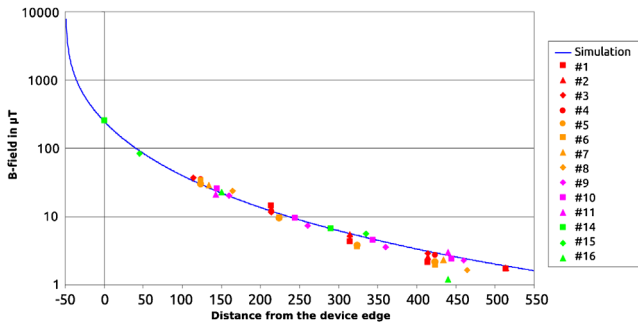
Fig. 4. Simulated B-field in front of the model of the generic cooking zone normalized to a B-field amplitude of 6.25 μT at a distance of 300 mm from the cooktop edge (50 mm from the rim of the generic cooking zone). Measured results are scaled to match amplitude and slope.

by the generic model was assessed as 17% (1.4 dB; Supplementary Table IV).

DOSIMETRIC RESULTS

Induced Current Density for the Generic Cooking Zone Model

Figure 5 shows the normalized peak average current density for the six non-pregnant models as a function of the distance from the generic cooking
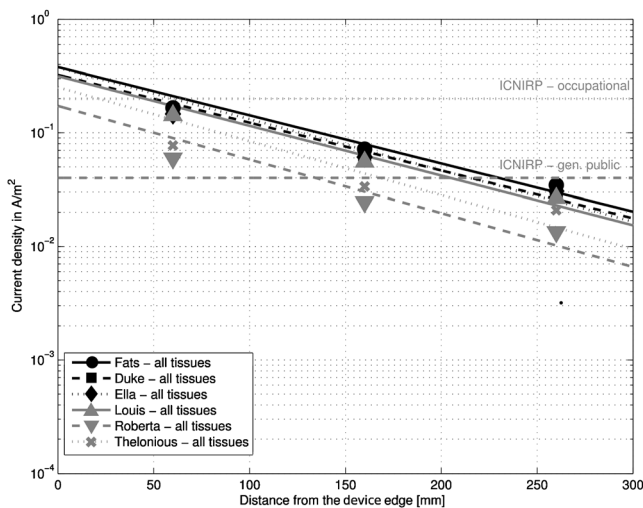

Fig. 5. Peak average current densities of all non-pregnant models in all body tissues normalized to the B-field of 6.25 μT at a distance of 300 mm from the cooktop edge (50 mm from the rim of the generic cooking zone). Symbols represent the simulation results at the different positions and the lines show exponential curve fits. Closest distance at which the current densities were evaluated is 10 mm from the rim of the cooking zone. This result has been included in the exponential curve fit but is outside the scope of the x-axis (−50 mm) of this figure and Figures 6–8.

zone model. For the definition of the distance reference, a spacing of 50 mm between the rim of the cooking zone and the front edge of the cooktop is assumed. No additional space between the cooktop edge and the cabinet edge is added, which is a valid assumption for typical stand-alone devices. The current of the cooking zone was normalized to a B-field strength of 6.25 μT at a distance of 300 mm from the cooktop edge (i.e., 450 mm from the center point of the cooking zone). Like this, the generic cooking zone corresponds to a worst-case device that is compliant with the exposure limits for the general public when tested according to IEC 62233.

At the operational frequency of 20 kHz, the limit for the induced current averaged over 1 cm^2 is 40 mA/m^2 for the general public and 200 mA/m^2 for occupational exposure. When considering the currents in all body tissues, the exposure limits for the general public are reached at distances between 200 and 250 mm for the adult models, and the abdominal region is the most exposed. For very close distances (<50 mm), even the occupational limits can be exceeded. The current density maxima typically occur in tissues with comparatively high conductivity such as muscle, the penis, or walls of the gall bladder or small intestine. The maxima are not necessarily located at the closest location to the cooking zone model. For the two models of the children whose heads directly face the cooking zone model, the current density maximum can also occur in the vitreous humor. The current density of the two child models is about a factor of 2 below the values observed for the adults in their abdominal regions. Supplementary Table III lists those tissues in which the current density maxima are typically observed, together with their conductivities at 20 kHz.

The current density in the CNS of the adult and adolescent models is approximately a factor of 10 below the current density averaged over all tissues for all observed cases (Fig. 6). Even when standing directly at the cabinet edge the basic restrictions are not reached. For these exposure conditions, the current density maximum is located in the lower part of the spinal cord, which is at a comparatively large distance from the coil. For young children whose heads are at the same height as the cooktop, the basic restrictions for the general public are violated at distances below 60 mm, with the current density maximum located in the brain. When standing immediately at the cooktop, the current densities in the CNS can exceed the basic restrictions by approximately a factor of 2. For the models of the pregnant woman and fetus, the averaged current density is shown in Figure 7. Among the investigated cases,
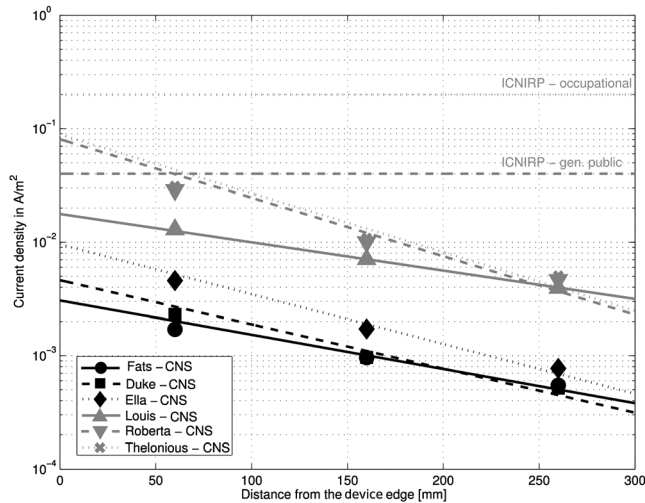
Fig. 6. Peak average current densities of all non-pregnant models in the CNS tissues normalized to the B-field of 6.25 μT at a distance of 300 mm from the cooktop edge (50 mm from the rim of the generic cooking zone). Symbols represent the simulation results at the different positions and the lines show exponential curve fits.

mother and fetus suffer the highest exposure in the 9th gestational month. The current density maximum typically occurs in the tissue of the uterus because of its high conductivity (Supplementary Table III). Current densities in the tissue of the mother model, immediately at the edge of the cooktop, are approximately a factor of 16 above the ICNIRP limit for the

general public when considering all tissues. With the exception of the fetus in the 3rd gestational month, the current densities in the fetal tissue reach limits for the general public at 100–170 mm when averaging over the entire body and exceed them by up to a factor of 6 at the cooktop edge. If only the CNS tissue is considered, the limits are a factor of 2.5 below the basic restrictions for the general public (Fig. 8). Considering the exposure of pregnant women in working environments, it is debatable whether the occupational limits or the limits for the general public should be applied to protect the fetus. Scaling the results of Figure 8 to a device that is only compliant with the occupational B-field limits (30.7 μT at 300 mm distance), shows that the exposure of the CNS tissue of the fetus can exceed the exposure limits for the general public if the mother is exposed in an occupational environment. It should, however, be noted that the brains of the fetus models are not oriented toward the cooking zone (Fig. 2 in the Online Supplementary Material). The exposure of the hand above the cooking zone almost reaches the occupational limit at distances from 50 mm above the cooking zone (Fig. 9), both for centered position and above the rim.

Normalization to the B-Field Amplitudes of the Measured Devices

In order to assess the exposure in persons in the close environment at the B-field levels of the different induction cooktops discussed above and in
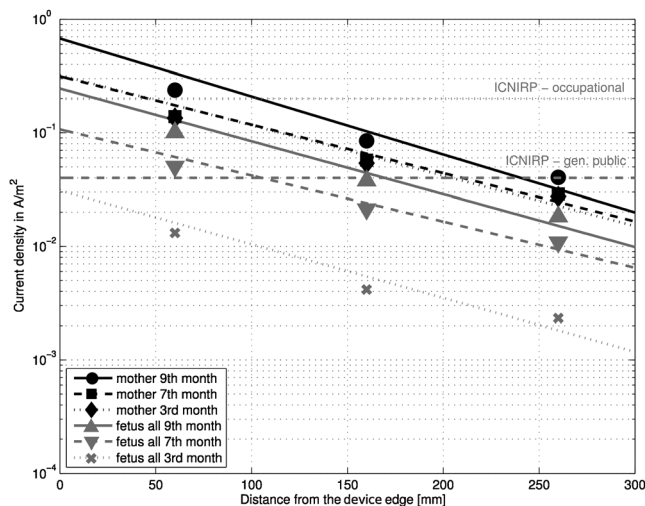

Fig. 7. Peak average current density of the pregnant models in the three gestational phases and the fetuses over all body tissues, normalized to the B-field of 6.25 μT at a distance of 300 mm from the cooktop edge (50 mm from the rim of the generic cooking zone). Symbols represent the simulation results and the lines show exponential curve fits.
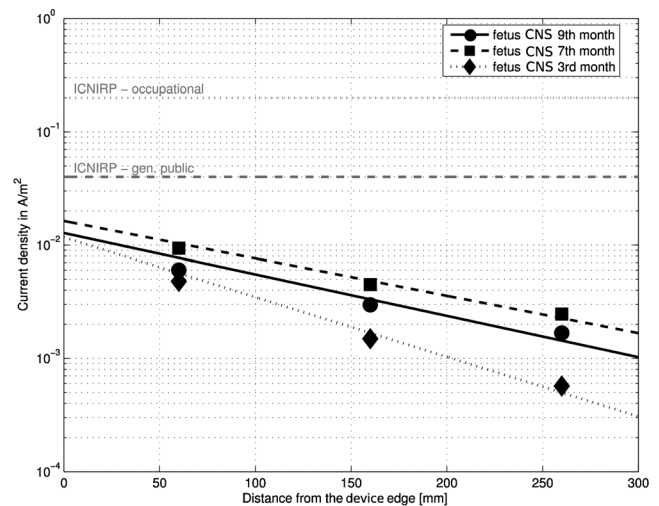

Fig. 8. Peak average current density in the CNS tissues of the fetuses normalized to the B-field of 6.25 μT at a distance of 300 mm from the cooktop edge (50 mm from the rim of the generic cooking zone). Symbols represent the simulation results and the lines show exponential curve fits.
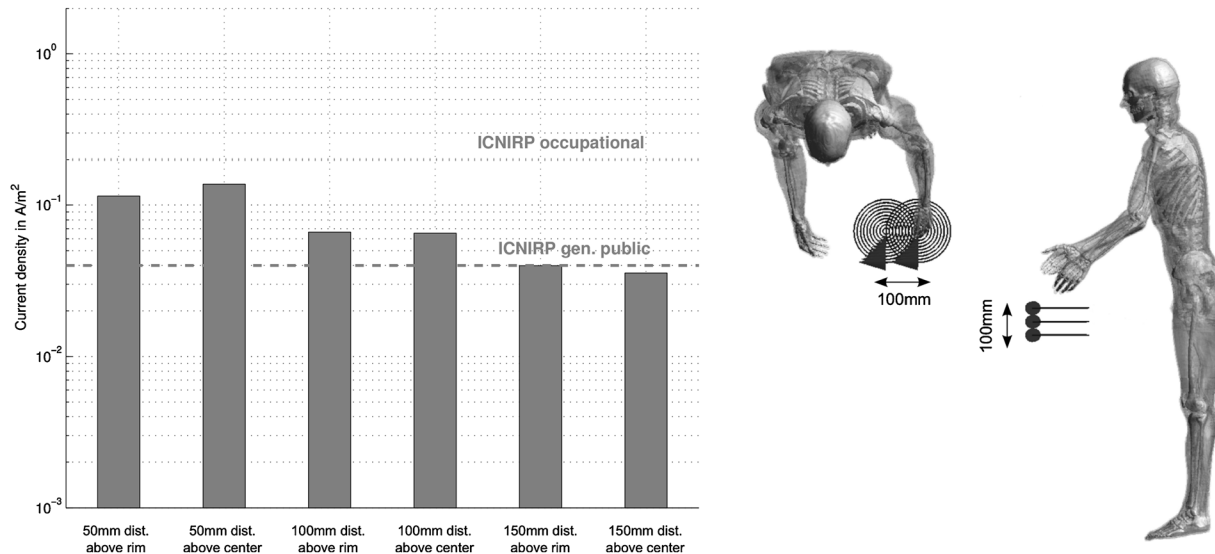
Fig. 9. Peak average current density in the hand of the model "Duke" at different distances and positions above the hobs normalized to the B-field of 6.25 μT at 300 mm from the edge of the generic cooktop.

Viellard et al. [2006], the exponential fit shown in Figures 5–8 was used to correlate the averaged current density maximum with the measurement results. The field strengths at the particular distances to the rims of the cooking zones were derived by normalizing these current densities with the scaling factors derived above. In addition, the increase in field strength for worst-case loading conditions was applied (Supplementary Table II). Figure 10 shows the exposure average of the anatomical models for which the maximum current density was observed for the generic cooking zone (Figs. 5–8), normalized to the

incident B-fields of the measured devices at three different distances. At 30 mm from the cabinet edge, parts of the user's body are assumed to protrude above the cabinet; at the cabinet edge, the user is assumed to touch the cabinet without any protruding regions of his body; and 300 mm from the cabinet edge is the maximum distance at which the fields were measured (this distance is regarded as typical for bystanders).

Figure 5 shows that the exposure of the non-pregnant models at the largest distance (300 mm from the cabinet) is always compliant with the basic
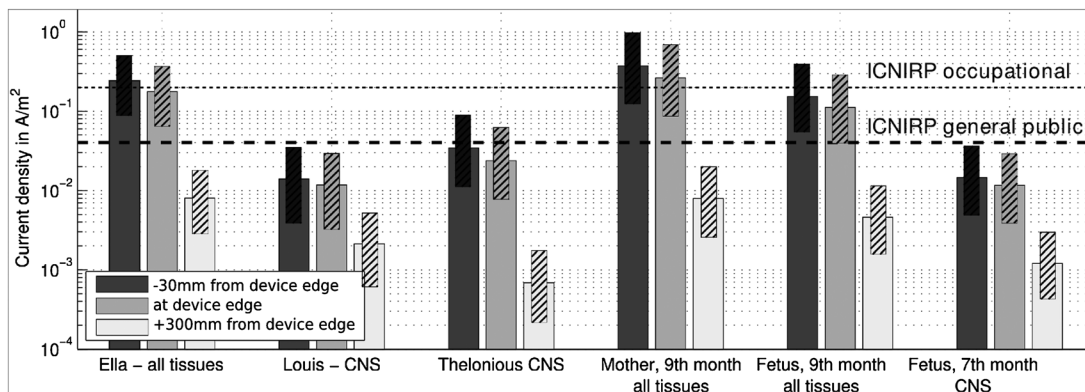

Fig. 10. Peak average current density in the CNS and all tissues of the anatomical models (most relevant cases of this figure and Figs. 8 and 9), normalized to the average of the measured devices at −30, 0, and 300 mm from the edge of the device. Hatched bars indicate the range from the best-to the worst-case device. Expanded uncertainty ($k = 2$) of the measurement and simulation results is 6.0 dB for the models of the adults and children (Supplementary Table V), and 6.4 dB for the fetus models (Supplementary Table VI).

restrictions for the general public even when including all body tissues for the current averaging. At close distances, the exposure limits for the general public can be exceeded by more than a factor of 5 (distance < 50 mm; Fig. 5). When considering CNS tissues only, the basic restrictions for the general public can be reached for the child models (Thelonious and Roberta) at close distances from the cabinet edge when allowing for the overall uncertainty of this evaluation. The combined numerical and experimental uncertainty was assessed as 6.0 dB ($k = 2$; Supplementary Table V) or as 0.50–2.0 of the provided exposure with a confidence interval of 95%.

The exposure of the mother and fetus models exceeds the basic restrictions for the general public by a factor of 6 for the mother and 3.5 for the fetus when standing at the cabinet edge, if considering all body tissues. Given the numerical and experimental uncertainty, the violation of the occupational limits can be regarded as likely for the devices with high B-fields. For CNS tissues of the fetus, the induced current density can reach the order of magnitude of the basic restrictions when taking into account the uncertainty. The combined numerical and experimental uncertainty for the exposure of the fetus was assessed as 6.4 dB ($k = 2$; Supplementary Table VI) or as 0.48–2.1 of the provided exposure with a confidence interval of 95%. In general, the current density reported by Kos et al. [2011] lies in the order of magnitude of the results shown in Figure 10. However, a direct comparison is difficult because the cooktops analyzed by Kos et al. [2011] operate at 35 kHz whereas the nominal frequency of all cooktops considered in this study is 20 kHz.

DISCUSSION AND CONCLUSIONS

The measured B-fields of 13 professional induction cooktops and the three domestic devices evaluated in Viellard et al. [2006] were evaluated experimentally. The field strengths are compliant with exposure limits for the general public when measured at 300 mm from the cooktops as specified by IEC 62233 [IEC, 2005]. Due to the high field gradients, the measured B-fields reach—or violate—the occupational exposure limits at short distances from the cooking zone. The current densities induced in the human body were modeled using a generic worst-case cooking zone model and different anatomical models including adults, pregnant women, and children. The current densities reached the exposure limits according to the ICNIRP 1998 guidelines for the general public at 300 mm from the cooktop. The results were then scaled to the measured B-field

levels of the professional and domestic cooktops. The findings can be summarized as follows: Most of the measured cooktops are compliant with the field limits for public exposure at a distance of 300 mm from the cooktop. Due to the high field gradients in the close environment of the cooking zone, most devices exceed these limits at closer distances. When considering the entire body of the exposed user for the current density averaging, the basic restrictions of the current density for the general public can be significantly exceeded and reach occupational levels. A generic worst-case cooktop which is compliant at the measurement distance specified by IEC 62233 can lead to current densities that exceed the basic restrictions for the general public by a factor of 16. The brain tissue of young children can be overexposed by a factor of 2 with respect to the basic restrictions for the general public if they come close to the cooktop. If exposure limits of the general public apply to the fetus of a mother in a working environment, the current density in the CNS tissue of the fetus can exceed the basic restrictions while they are still fulfilled for the mother.

To summarize, the IEC 62233 standard does not sufficiently protect exposed persons according to the basic restrictions defined by the ICNIRP 1998 guidelines, which are enforced in many countries. The high field gradients in the close environment of induction cooktops need be considered very carefully. It should be noted that a recent ICNIRP statement defines different basic restrictions in terms of the electric field in the entire body and proposes higher reference levels for the incident B-field [ICNIRP, 2010]. Electric field limits have already been established by the IEEE [2002]. Because of the large differences in the dielectric properties of body tissues, the maxima of the current density and the electric field strength are not directly correlated.

REFERENCES

Capstick M, McRobbie D, Hand J, Christ A, Kühn S, Hansson Mild K, Cabot E, Li Y, Melzer A, Papadaki A, Prüssmann K, Quest R, Rea M, Ryf S, Oberle M, Kuster N. 2008. An Investigation into Occupational Exposure to Electromagnetic Fields for Personnel Working With and Around Medical Magnetic Resonance Imaging Equipment. EU Commission Study on MRI (Project VT/2007/017). IT'IS Foundation: Zürich, Switzerland. http://www.itis.ethz.ch/assets/Downloads/Papers-Reports/Reports/VT2007017FinalReportv04.pdf (Last accessed 14 March 2012).

Christ A, Schmid G, Djafarzadeh R, Überbacher R, Cecil S, Zefferer M, Neufeld E, Lichtsteiner M, Bouterfas M, Kuster N. 2009. Numerische Bestimmung der Spezifischen Absorptionsrate bei Ganzkörperexposition von Kindern:

Abschlußbericht. (Numerical evaluation of the specific absorption rate of children under whole-body exposure: Final report.). IT'IS Foundation: Zürich, Switzerland. http://www.emf-forschungsprogramm.de/www/home/akt_emf_forschung.html/dosi_HF_003_ZwB_01.pdf (Last accessed 17 April 2012).

Christ A, Kainz W, Hahn EG, Honegger K, Zefferer M, Neufeld E, Rascher W, Janka R, Bautz W, Chen J, Kiefer B, Schmitt P, Hollenbach HP, Shen J, Oberle M, Szczerba D, Kam A, Guag JW, Kuster N. 2010. The Virtual Family—Development of surface-based anatomical models of two adults and two children for dosimetric simulations. Phys Med Biol 55:N23–N38.

Dawson TW, Caputa K, Stuchly MA. 1997. A comparison of 60 Hz uniform magnetic and electric induction in the human body. Phys Med Biol 42:2319–2329.

Dimbylow P. 2008. Quandaries in the application of the ICNIRP low frequency basic restriction on current density. Phys Med Biol 53:133–145.

Gabriel S, Lau RW, Gabriel C. 1996. The dielectric properties of biological tissues: III. Parametric models for the dielectric spectrum of tissues. Phys Med Biol 41:2271–2293.

Gandhi OP, Chen JY. 1992. Numerical dosimetry at power-line frequencies using anatomically based models. Bioelectromagnetics 13(Suppl. 1):S43–S60.

ICNIRP. 1998a. Guidelines for limiting exposure to time-varying electric, magnetic and electromagnetic fields (up to 300 GHz). Health Phys 74:494–522.

ICNIRP. 1998b. Response to questions and comments on the guidelines for limiting exposure to time-varying electric, magnetic and electromagnetic fields (up to 300 GHz). Health Phys 75:438–439.

ICNIRP. 2010. ICNIRP Statement—Guidelines for limiting exposure to time-varying electric and magnetic fields (1 Hz to 100 kHz). Health Phys 99:818–836.

IEC. 2005. Standard 62233. Measurement methods for electromagnetic fields of household cooktops and similar apparatus with regard to human exposure, 106/99, Final Draft International Standard, Brussels, Belgium.

IEEE. 2002. C95.6. IEEE standard for safety levels with respect to human exposure to electromagnetic fields, 0–3 kHz. IEEE Standards Department, International Committee on Electromagnetic Safety. The Institute of Electrical and Electronics Engineers, New York, NY, USA.

Kos B, Valič B, Miklavčič D, Kotnik T, Gajšek P. 2011. Pre- and post-natal exposure of children to EMF generated by domestic induction cookers. Phys Med Biol 56:6149–6160.

Kromeyer-Hauschild L, Wabitsch M, Kunze D, Geller F, Geiß HC, Hesse V, von Hippel A, Jaeger U, Johnsen D, Korte W, Menner K, Müller G, Müller JM, Niemann-Pilatus A, Remer T, Schaefer F, Wittchen HU, Zabransky S, Zellner K, Ziegler A, Hebebrand J. 2001. Perzentile für den Body-mass-Index für das Kindes und Jugendalter unter Heranziehung verschiedener deutscher Stichproben (Percentiles for the body mass index for childhood and adolescence with reference to several German random samples). Monatsschr Kinderheilkd 149:807–818.

Levine D. 2005. Atlas of fetal MRI. Boca Raton, FL: Taylor & Francis.

Liu F, Zhao H, Crozier S. 2003. On the induced electric field gradients in the human body for magnetic stimulation by gradient coils in MRI. IEEE Trans Biomed Eng 50:804–815.

Orcutt N, Gandhi OP. 1988. A 3-D impedance method to calculate power deposition in biological bodies subjected to time varying magnetic fields. IEEE Trans Biomed Eng 35:577–583.

Petoussi-Henss N, Zankl M, Fill U, Regulla D. 2002. The GSF family of voxel phantoms. Phys Med Biol 47:89.

Taflove A, Hagness SC. 2000. Computational electromagnetics: The finite-difference time-domain method, 2nd edition. Boston, USA, London, UK: Artech House.

Viellard C, Romann A, Lott U, Kuster N. 2006. B-field exposure from induction cooking appliances, Technical Report. IT'IS Foundation: Zürich, Switzerland. http://www.bag.admin.ch/themen/strahlung/00053/00673/03156/index.html?lang=de&download=M3wBPgDB/8ull6Du36WenojQ1NTTjaXZnq-WfVpzLhmfhnapmmc7Zi6rZnqCkkIZ3fnyDbKbXrZ6lhu-DZz8mMps2gpKfo (Last accessed 14 March 2012).

Yamazaki K, Kawamoto T, Fujinami H, Shigemitsu T. 2004. Equivalent dipole moment method to characterize magnetic fields generated by electric appliances: Extension to intermediate frequencies of up to 100 kHz. IEEE Trans Electromagn Compat 46:115–120.